Study of Thrombin-Derived C-Terminal Peptide with aggregation propensity

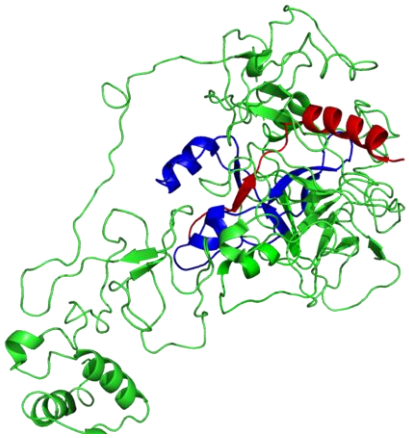

Author: Klaudia Detkiewicz
Supervisor: Ganna Petruk

Bachelor's Degree Project, 15 ECTS
Autumn Term 2021, MOBK01

Department of Biology, Lund University

Department of Clinical Sciences, Division of Dermatology and Venereology, Lund University

Abstract

Skin wounds are always at risk of contamination by different microbe species. When pathogens multiply and overcome the body's immune system, local infection occurs. This, in turn, can turn into a systemic infection and lead to sepsis that can result in death. The drugs available on the market to combat such scenarios are mainly antibiotics. Unfortunately, most of them are rapidly losing their effectiveness due to the growing problem of antibiotic resistance. Recently, in Schmidtchen lab, it was discovered that a naturally existing protein in the body, thrombin, also has other functions besides its role in blood clotting. Indeed, after the cleavage of thrombin with human neutrophil elastase (HNE), several fragments of different lengths found in wound fluids, are released from the C-terminal region. Thrombin-derived C-terminal peptides (TCPs) of roughly 2 kDa have shown strong antimicrobial and anti-inflammatory activity, while peptides of 11 kDa have displayed a propensity to aggregate endotoxins. In this work, recombinant 11-kDa TCP (called rTCP96) was produced, employing E. coli expression system. The peptide was purified exploiting His-tag through affinity chromatography. Then, its secondary structure and ability to aggregate bacteria were evaluated, using circular dichroism and Live/Dead assay, respectively. Indeed, it was shown that rTCP96 has the propensity to aggregate bacteria.

Table of contents:

1. Introduction……...4

2. Aim of the thesis……..…5

3. Materials and methods……..….5

3.1 Expression of His-tagged rTCP96……..…..…5

3.2 Purification of His-tagged rTCP96…….…..….6

3.3 SDS-PAGE and Western blot……..…….6

3.4 Circular Dichroism spectroscopy…….…….6

3.5 Live/Dead assay…….....7

4. Results…….….8

4.1 Purification of His-tagged rTCP96……..8

4.2 Purity and specificity of purified rTCP96…….....9

4.3 Secondary structure of rTCP96 and its structural change when bound to LPS……...9

4.4 rTCP96 aggregates bacteria……10

5. Discussion……...11

6. Conclusions……12

7. Acknowledgment……...12

8. References…….…….13

9. Appendix……..……..15

1. Introduction

Skin wounds are always at risk of contamination by microbes of various species. The most common of them are *Staphylococcus aureus*, *Pseudomonas aeruginosa*, and *Escherichia coli* (Berríos-Torres et al., 2017). The excessive presence of microbes in the wound region and their virulence overwhelming the host defense may lead to chronic inflammation and inability to heal the wound (Bowler et al., 2001; Rahim et al., 2017). According to the World Health Organization, antibiotic resistance is a global problem that has been estimated to be one of the biggest public health challenges of our time (WHO, 2020). It requires quick actions and finding new alternatives for antibiotics since they are losing their efficacy.

One of the host defense mechanisms against microbes contaminating wounds is antimicrobial peptides (AMPs). They are produced by all organisms beginning from prokaryotes and ending on humans (Hancock & Sahl, 2006). In addition to their role in the host defense against microbes, they are involved in other actions such as modulation of inflammatory and immune responses and promoting wound healing (Gera et al., 2021). Due to the multiple activities of AMPs and their low susceptibility to bacterial resistance evolution, the antimicrobial peptides may constitute potential broad-spectrum antibiotics and anti-biofilm agents (Gera et al., 2021).

Thrombin is a serine protease that is involved in blood clotting. It is produced as a proenzyme called prothrombin (72 kDa) that, after the cleavage, becomes an active enzyme (36 kDa). The role of thrombin is to convert soluble fibrinogen into insoluble fibrin and to catalyze other steps involved in blood coagulation (Widmaier et al., 2018). Recently, in Schmidtchen lab, it was discovered that thrombin can also have another function. Indeed, it was shown that after proteolysis of thrombin with human neutrophil elastase (HNE), several fragments of different lengths, found in wound fluids, are released from the C-terminal region (*Figure 1*) (van der Plas et al., 2016; Holdbrook et al.,2018). Thrombin-derived C-terminal peptides (TCPs) of roughly 2 kDa (Papareddy et al., 2010) have shown strong antimicrobial and anti-inflammatory activity, both *in vitro* and *in vivo* (van der Plas et al., 2016; Holdbrook et al., 2018; Papareddy et al., 2010; Kasetty et al., 2011; Kalle et al., 2012; Puthia et al., 2020), while, peptides of around 11 kDa were shown to aggregate in the presence of LPS and *E. coli* (Petrlova et al., 2017). These latest data suggest that the longer TCPs, through aggregation, may play a key role in controlling bacterial infections and reducing lipopolysaccharide (LPS)-induced inflammation. Nevertheless, if the protein aggregation can be considered as a fundamental innate defense mechanism, is at present unknown. Therefore, it would be of great value to understand if 11 kDa TCPs are able to aggregate also other bacteria than *E. coli*. This information will give us new insights on the physiological roles of aggregation, studies that could lead to the development of new therapeutics based on TCPs that could prevent excessive inflammatory activations induced by bacterial infections.

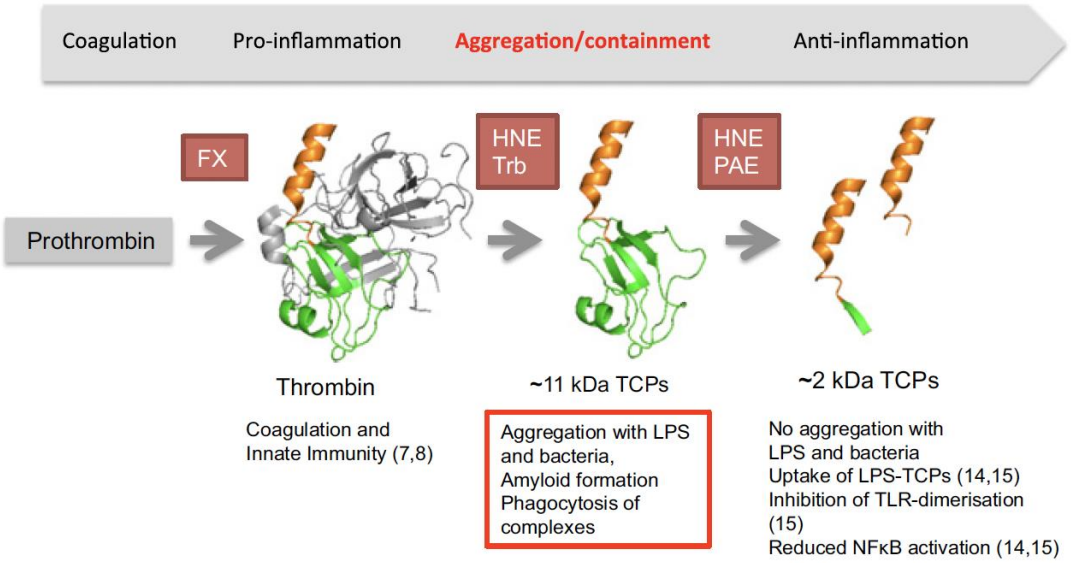

Figure 1: Schematic illustration for multiple functions of thrombin and its fragments. *Retrieved from (Petrlova et al., 2017).*

2. Aim of the thesis

The aims of this thesis are:

1. Produce recombinantly 11-kDa TCP (called rTCP96) using *E. coli* expression system;
2. Purify the peptide from bacterial extract through affinity chromatography;
3. Evaluate the peptide's secondary structure by circular dichroism;
4. Investigate its ability to aggregate bacteria using Live/Dead assay.

3. Material and methods

3.1 Expression of His-tagged rTCP96

Recombinant Thrombin-derived C-terminal Peptides (rTCP96) was produced using a bacterial expression system consisting of pGEX plasmid in *Escherichia coli* strain BL21 codon plus (DE3) RIPL (Invitrogen). pGEX plasmid carried genes for the TCP96 equipped with polyhistidine-tag (His-tag) and contained the T7 RNA polymerase gene under the control of the LacUV5 promoter. Bacteria were cultivated in Luria Bertani (LB) medium supplemented with antibiotics: chloramphenicol (34 µg/mL) and carbomycin (100 µg/mL). Bacteria grew at 37 °C with vigorous shaking until optical density at 620 nm (OD_{620}) reached a value of 0.6 OD. Expression of rTCP96 was induced by adding 0.25 mM Isopropyl β- d-1-thiogalactopyranoside (IPTG) to the medium with bacteria and stopped after 3h of incubation at 37 °C with vigorous shaking. Then, bacteria were harvested by centrifugation (4000 *g* for 15 min), washed with 10 mM Tris at pH 7.4 and pellet was stared at –20 °C until purification.

3.2 Purification of His-tagged rTCP96

To purify rTCP96, the pellet deriving from 0.5 L of bacterial culture was resuspended in 10 mL of 10 mM Tris at pH 7.4 containing 8 M urea and 20 mM imidazole (lysis buffer). Afterwards, the cells were disrupted by sonication (10 sec ON and 10 sec OFF, 10 times) and the soluble fraction, containing the peptide of interest, was separated from the cell debris by centrifugation (4000 *g* for 20 min). Finally, the supernatant was filtered with a 0,22 µm syringe filter and diluted with other 10 mL of lysis buffer.
The His-tagged peptide was purified by Immobilized Metal Affinity Chromatography (IMAC) (His-Trap-Nickel-chelating columns, GE Healthcare) under denaturing conditions (8 M urea in 10 mM Tris at pH 7.4). Proteins with low affinity to the column were washed off with the wash buffer (8 M urea, 20 mM imidazole, in 10 mM Tris at pH 7.4). The peptide of interest bound to the column was eluted by adding elution buffer (8 M urea, 200 mM imidazole in 10 mM Tris at pH 7.4). First 5 fractions were collected in Eppendorf tubes (500 µL each). The concentration of rTCP96 and absorbance at 280 nm of collected fractions were determined using NanoDrop™ (ND 1000, Thermo Scientific). Fractions containing rTCP96 were reunited, diluted with lysis buffer 1:1 and dialyzed stepwise in 10 mM Tris at pH 7.4 to prevent protein aggregation. To allow the peptide to acquire physiological folding, the dialysis was conducted at 4 °C.

3.3 SDS-PAGE and Western blot

To assess the purity and the specificity of the eluted peptide SDS-PAGE followed by Coomassie staining or western blot were used, respectively. 10 µl of lysate, flow through, or 2 µg of eluted fractions containing rTCP96 were mixed (1:1) with loading buffer containing reducing agent (Dithiothreitol, DTT). Subsequently, the samples were denatured at 95°C for 5 minutes and loaded on a 10–20% Novex Tricine pre-cast gel (Invitrogen, Carlsbad, CA, USA). Electrophoresis was performed at 120 V for 90 min.
The gel was stained using Coomassie Brilliant blue (Invitrogen, Rockford, IL, USA), and images were obtained using a Gel Doc Imager (Bio-Rad Laboratories, Hercules, CA, USA). For western blotting, the material was subsequently transferred to a PVDF membrane using a Trans-Blot Turbo system (Bio-Rad, Laboratories, Hercules, CA, USA). rTCP96 was detected using polyclonal rabbit antibodies against the C-terminal thrombin epitope VFR17 (VFRLKKWIQKVIDQFGE; diluted 1:1000, Innovagen AB, Lund, Sweden), followed by porcine anti-rabbit HRP conjugated antibodies (1:1000, Dako, Glostrup, Denmark). The peptide was visualized by incubating the membrane with SuperSignal West Pico Chemiluminescent Substrate (Thermo Scientific, Rockford, IL, USA) for 5 min, followed by detection using a ChemiDoc XRS Imager (Bio-Rad Laboratories, Hercules, CA, USA).

3.4 Circular Dichroism spectroscopy

The secondary structure of rTCP96 was investigated using Circular Dichroism (CD). The measurements were performed on a Jasco J-810 spectropolarimeter (Jasco, USA) equipped with a Jasco CDF-426S Peltier set to 25 °C. A cuvette with a light path of 0,2 cm (Hellma, GmbH & Co, Germany) was used for all measurements. Each measurement was repeated three times in far UV spectra of 190-260 nm, a scan speed of 20 nm/min, and a bandwidth of 1 nm. For measurements, 5 µM of rTCP96 in 10 mM Tris at pH 7.4 alone, or after incubating it with 100 µg/mL *E. coli* lipopolysaccharides (LPS) at 37 °C for 30 minutes, was used. For comparison, the

secondary structure of 10 µM TCP-25, C-terminal fragment of 25 amino acids of rTCP96, with and without LPS was also investigated. Raw spectra were corrected for buffer contribution and converted to the mean residue ellipticity, θ (mdeg cm^2 $dmol^{-1}$) following the equation:

$$Molar\ ellipticity = \frac{\theta 222 \times \frac{Mw}{aa}}{10 \times c \times l}$$

where θ222 = observed ellipticity at 222 nm in millidegrees, Mw = molecular weight of the protein in Da, aa = number of amino acids, c = concentration in mg/mL, l= path length of the cuvette in cm.

The α-helical content in protein structure was calculated using the following equation:

$$\alpha - helical\ content = \frac{(\theta 222 + 3000)}{(-39000 + 3000)}$$

where 3000 and –39000 are constants based on the helicity of poly-L-lysine (Greenfield and Fasman, 1969). Smoothed graphs of all measurements were used for analysis.

3.5 Live/Dead assay

To evaluate the ability of rTCP96 to aggregate bacteria LIVE/DEAD® BacLight™ Bacterial Viability kit (Invitrogen, Molecular Probes, Carlsbad, CA) was used. Two different strains of bacteria, *S. aureus* ATCC 29213 (Gram-positive) and *P. aeruginosa* ATCC 27853 (Gram-negative) were used. Briefly, bacteria were cultured overnight in 5 mL of Todd-Hewitt (TH) medium at 37°C with vigorous shaking. Then 100 µL of the overnight cultures were added to 5 mL fresh TH-media and incubated in the same conditions until OD_{620} of 0.4 was reached. Then, bacteria were centrifuged at 5000 RPM for 10 minutes at room temperature and the pellet was washed with 5 mL 10 mM Tris at pH 7.4. Subsequently, the pellet was diluted with 10 mM Tris at pH 7.4 so that the total amount of bacteria was $2 \cdot 10^8$ CFU/mL. Bacteria (2 x 10^6 CFU/mL) were incubated with rTCP96 (5 µM) at 37 °C for 2 h. Buffer (10 mM Tris in HCl at pH 7.4) alone was used as a negative control and TCP-25 (5µM) as a positive control. At the end of incubation, samples were mixed 1:1 with a staining solution containing 3 µL of component A (SYTO®9 green-fluorescent nucleic acid stain) and 3 µL of B (red-fluorescent nucleic acid stain propidium iodide) dissolved in 2 mL of 10 mM Tris pH 7.4. Then the samples were incubated in the dark at room temperature for 15 min and spun down at 14 000 RPM for 5 min. Almost all supernatant was discarded and the pellet was resuspended in the remaining volume. Next, 5 µL of each stained bacterial suspension was transferred onto a slide and covered with an 18-mm square coverslip. Zeiss AxioScope A.1 fluorescence microscope was used to analyze three independent sample preparations. Objectives: Zeiss EC Plan-Neofluar x20 and x40 were used for analysis and representative pictures were taken.

4. Results

4.1 Purification of His-tagged rTCP96

rTCP96 was purified through immobilized-metal affinity chromatography exploiting its His-tag. The concentration of rTCP96 in eluted fractions was measured using NanoDrop™ (ND 1000, Thermo Scientific). The results are presented in *Table 1*. Elution profile of rTCP96 was done using data from Nanodrop and is reported in *Figure 2*. Protein expression and purification were performed two times. Data from one representative experiment is shown.

Table 1: Concentration of rTCP96 in eluted fractions measured by NanoDrop™.

N. of fraction	Absorbance at 280 nm	Concentration (mg/mL)
1	0,643	0,366
2	0,350	0,199
3	0,086	0,049
4	0,033	0,019
5	0,016	0,009

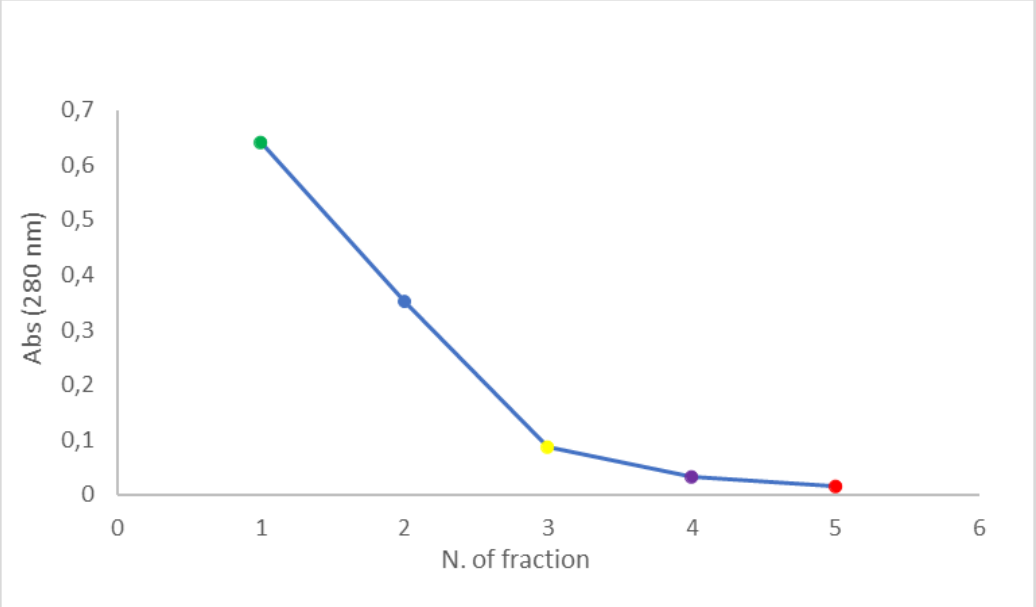

Figure 2: Elution profile of rTCP96 obtained after eluting the peptide from the column. *x-axel indicates the number of eluted fractions and y-axel indicates absorbance at 280 nm.*

Fractions 1-3 were reunited and theoretical concentration was calculated as in Appendix.

After all purification steps, the final amount of rTCP96 was around 0,42 mg/L of bacterial culture and the purification yield after dialysis was around 68%.

4.2 Purity and specificity of purified rTCP96

Protein purity and specificity in the eluted samples was estimated by SDS-PAGE followed by Coomassie blue staining and western blot, respectively. Results are shown in *Figure 3*.
As expected, several bands in both lysate and flow through (Figure 3a, lane 2 and 3, respectively), indicating the presence of different proteins, were observed. While eluted fractions showed mainly bands corresponding to the molecular weight of rTCP96 and one at around 32 kDa, suggesting an oligomerization of the peptide. (*Figure 3a, lane 4-6*).
Purification of rTCP96 was confirmed by western blot. As shown in *Figure 3b,* the bands at expected molecular weight were recognized by specific antibodies against C-terminal region of the peptide.

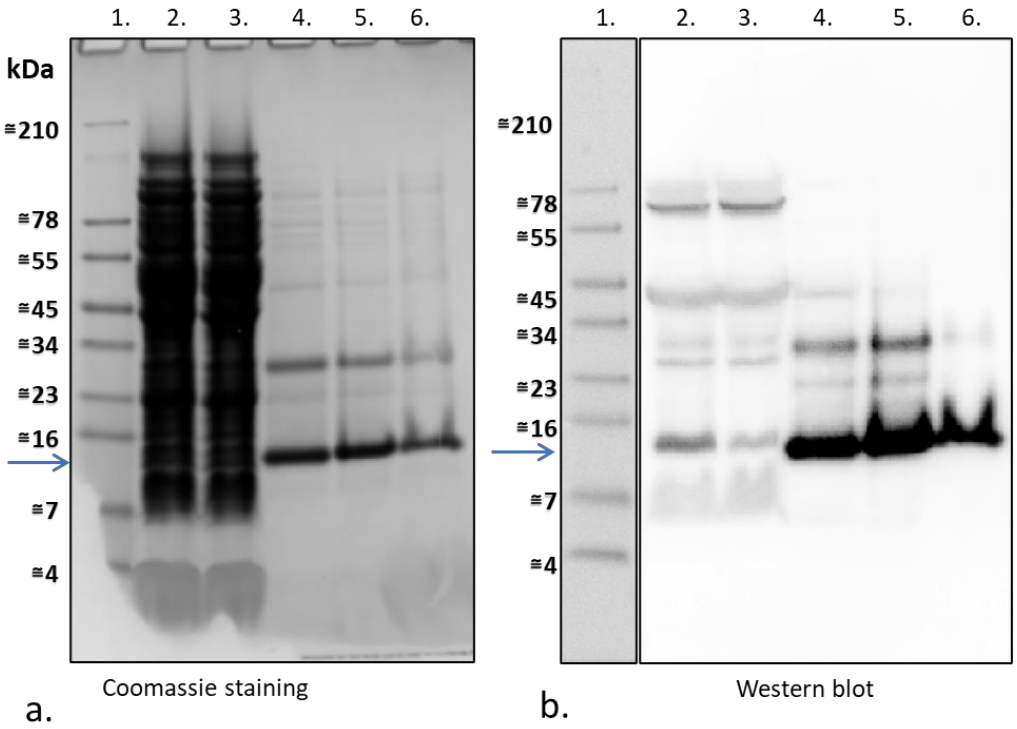

Figure 3: SDS-PAGE analysis of purified rTCP96 followed by Coomassie staining (a) or Western Blot (b)*. Loading order: 1. Pre-stained protein standard (STD), 2. Lysate (10 µL), 3. Flow through (10 µL), 4. Eluted fraction N. 1 (2 µg), 5. Eluted fraction N. 2 (2 µg), 6. Eluted fraction N. 3 (2 µg). Blue arrows indicate the molecular weight of rTCP96. One representative experiment is shown (n=2) .*

4.3 Secondary structure of rTCP96 and its structural change when bound to LPS

Circular Dichroism (CD) spectroscopy is a biophysical method that can determine the structure of small molecules based on the differential absorption of left and right circularly polarized light (Greenfield, 2006). Therefore, we employed this technique to assess the secondary structure of rTCP96 (5 µM) in the absence and the presence of 100 µg/mL LPS. TCP-25 was used for comparison. The result is presented in *Figure 4.* It was possible to observe a conformational

change in rTCP96 structure when LPS was added. It was previously shown that TCP-25 alone has an unstructured conformation, but when adding LPS, the peptide changes its shape to a typical α-helical structure (Papareddy et al., 2010). The same result was obtained during our experiments (*Figure 4*).

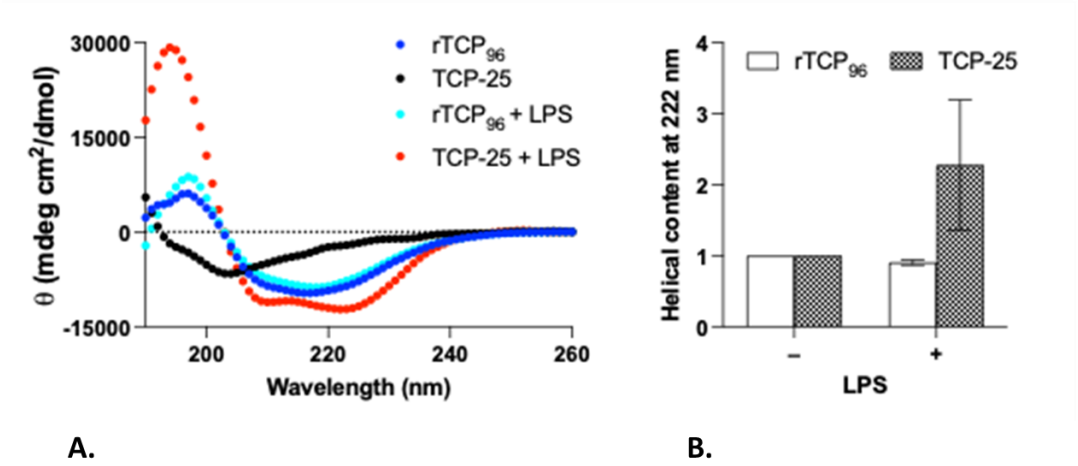

Figure 4: Structural changes of rTCP96 and TCP-25 upon binding to LPS. (A) *The secondary structure of rTCP96 (5 µM) alone and TCP-25 (10 µM) alone or after incubation with LPS (100 µg/mL) at 37°C for 30 minutes. Representative spectra of two different experiments are reported (n=2).* ***(B)*** *Helical content at 222 nm of rTCP96 (white) and TCP-25 (checkerboard) alone (–) or with LPS (+).*

4.4 rTCP96 aggregates bacteria

The ability of rTCP96 to aggregate bacteria was studied with Live/Dead assay. Peptides (rTCP96 or TCP-25) were incubated with *Pseudomonas aeruginosa* or *Staphylococcus aureus* for 2 h at 37 °C. Then bacteria were stained with a dye and observed under a fluorescence microscope. Bacteria incubated only with buffer were used as a control. The results are shown in *Figure 5*. As expected, controls consisted mainly of alive bacteria (green). Whereas in the samples with rTCP96, many aggregates containing both alive and dead (red) bacteria could be found. In the sample with TCP-25, there were no aggregates but only dead bacteria. Furthermore, the number of bacteria in this sample was lower than in other samples.

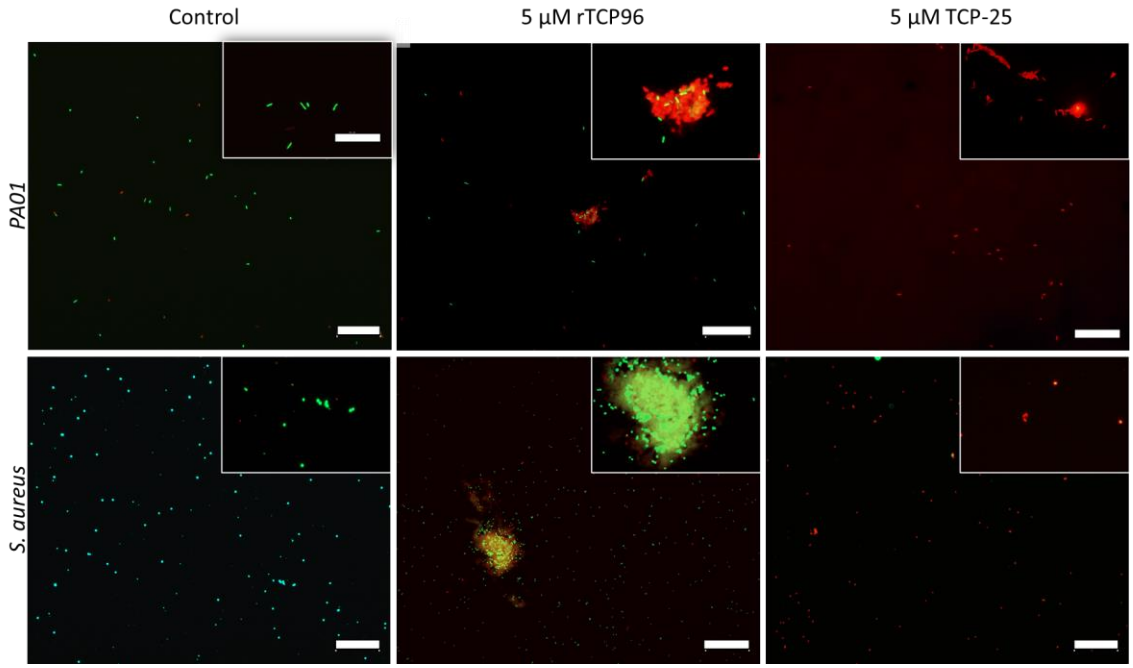

Figure 5: Visualization of live (green) and dead (red) bacteria using fluorescence microscopy. *Pseudomonas aeruginosa ATCC 27853 (PA01) and Staphylococcus aureus ATCC 29213 were incubated with 5 µM rTCP96 or 5 µM TCP-25 in 10 mM Tris at pH 7.4. The buffer alone was used as a control. Bacteria were stained with LIVE/DEAD® BacLight™ staining and visualized by fluorescence microscopy. The scale bar is 50 µm for all images and 20 µm for the inserts. One representative image from two independent experiments is shown (n=2).*

5. Discussion

The main goal of this thesis was to understand if recombinantly produced 11-kDa thrombin-derived C-terminal peptide (TCP) was able to aggregate other bacteria besides *E. coli*, such as *S. aureus* and *P. aeruginosa*.

Since the cost of thrombin´s peptides purified from human plasma is very high, we decided to express and purify the fragment of our interest (rTCP96) recombinantly, exploiting *E.coli* expression system. Generally, the yield of purified peptides from *E. coli* is around 1-50 mg/L of bacterial culture (Gaglione et al., 2017; Herbel et al., 2015; Pane et al., 2016), in our case we obtained a much lower amount (0.42 mg/L). There is a precise reason why the expression conditions have not been improved to achieve better production yield. Indeed, the isoelectric point of this peptide at pH 7.4 is very close to 0, this means that at this pH (corresponding to physiological pH) the peptide at higher concentrations in solution would form aggregates that would precipitate in amorphous structures (Xia, 2007).

The secondary structure of rTCP96 was evaluated by Circular Dichroism, both in the absence and in the presence of LPS. We could see that the peptide structure did change, suggesting the binding, even if the difference was not so visible as in the case of TCP-25. Indeed, TCP-25 after the addition of LPS switched from an unstructured form to a typical α-helical structure. These results agree well with what was reported before by Petrlova and colleagues (Petrlova et al., 2020). However, in their experiments, under the same conditions, the change in the secondary structure

of rTCP96 after LPS addition was more pronounced than in ours. This difference in results could be due to both the use of the different batch of peptide and LPS.

Even if rTCP96 showed a typical spectrum of β-sheet, with only CD experiments it is not possible to claim that the peptide aggregates and forms amyloid structures. To demonstrate this we should have done another experiment, such as Thioflavin T (ThT) assay, as reported by Petrlova (Petrlova et al., 2017 and 2020). ThT preferentially binds to the β-sheet structures of amyloidogenic proteins, indicating the formation of aggregates (Bolder et al., 2007).

Using Live/Dead staining we showed that purified rTCP96 was able to aggregate both *P. aeruginosa* and *S. aureus*. These results are in agreement with the results reported by Petrlova and colleagues (Petrlova et al., 2020). As shown previously, we could also see both green and red bacteria in the aggregates, indicating that rTCP96 not only aggregates bacteria but also kills them. This result was more visible in the samples with *P. aeruginosa*. This is not surprising, since it was demonstrated that rTCP96 has stronger antimicrobial activity on Gram-negative than on Gram-positive bacterial strains (Petrlova et al., 2020). However, from our Live/Dead assay, we could not estimate how many bacteria were killed by rTCP96. To illustrate this, we should have done the viable count assay, where after incubation with rTCP96 we should have plated the bacteria on TH-agar plates, let them grow overnight, and then count the colony-forming units (CFU) (Petrlova et al., 2020).

6. Conclusions

In summary, 11-kDa thrombin-derived C-terminal peptide (rTCP96) was expressed in *E. coli* system and purified through affinity chromatography with a satisfactory yield (0.42 mg/L of bacterial culture). The peptide has shown a conformational change upon incubation with LPS, suggesting a binding, and was able to aggregate both Gram-negative and Gram-positive bacteria. All these results were in agreement with findings reported by Petrlova and colleagues (Petrlova et al. 2017 and 2020).

7. Acknowledgment

I would like to express big gratitude to my supervisor Ganna Petruk from whom I have learned a lot. I am grateful for her great commitment to guiding me and coordinating my development. In addition, I would like to thank Arthur Schmidtchen for giving me the opportunity to join his team and everyone from the group of Arthur Schmidtchen for their help during this project. Last but not least, I would like to thank my family and friends for their faith in me and for being excellent support for me.

8. References

Alexander, C., Guru, A., Pradhan, P., Mallick, S., Mahanandia, N. C., Subudhi, B. B., & Beuria, T. K. (2020). MazEF-rifampicin interaction suggests a mechanism for rifampicin induced inhibition of persisters. *BMC molecular and cell biology*, *21*(1), 1-11. https://doi.org/10.21203/rs.3.rs-35194/v1

Alexander C., Rietschel E. (2001). Bacterial lipopolysaccharides and innate immunity. *Journal of Endotoxin Research, 7(3),* 167-202. https://journals-sagepub-com.ludwig.lub.lu.se/doi/pdf/10.1177/09680519010070030101

Berríos-Torres, S. I., Umscheid, C. A., Bratzler, D. W., Leas, B., Stone, E. C., Kelz, R. R., ..., Mazuski, J. E. (2017). Centers for Disease Control and Prevention Guideline for the Prevention of Surgical Site Infection, 2017. *JAMA Surgery*, *152*(8), 784-791. https://doi.org/10.1001/jamasurg.2017.0904

Bolder S., Sagis L., Venema P., van der Linden E. (2007). Thioflavin T and Birefringence Assays to Determine the Conversion of Proteins into Fibrils. *Langmuir 23,* 4144-4147. https://doi.org/10.1021/la063048k

Bowler, P., Duerden, B., Armstrong, D. G. (2001). Wound microbiology and associated approaches to wound management. *Clinical Microbiology Reviews*, *14*(2), 244-269. https://doi.org/10.1128/CMR.14.2.244-269.2001

Gera, S., Kankuri, E., & Kogermann, K. (2021). Antimicrobial peptides–Unleashing their therapeutic potential using nanotechnology. *Pharmacology & Therapeutics*, Article 107990. https://doi.org/10.1016/j.pharmthera.2021.107990

Greenfield, N. J., (2006). Using circular dichroism spectra to estimate protein secondary structure. *Nature Protocols*, *1*, 2876–2890. https://doi.org/10.1038/nprot.2006.202

Greenfield, N. J., Fasman, G. D., (1969). Computed circular dichroism spectra for the evaluation of protein conformation. *Biochemistry 8*(10), 4108–4116. https://doi.org/10.1021/bi00838a031

Hancock, R. E., & Sahl, H. G. (2006). Antimicrobial and host-defense peptides as new anti-infective therapeutic strategies. *Nature biotechnology*, *24*(12), 1551-1557. https://doi.org/10.1038/nbt1267

Herbel V., Schäfer H., Wink M. (2015). Recombinant Production of Snakin-2 (an Antimicrobial Peptide from Tomato) in E. coli and Analysis of Its Bioactivity. *Molecules, 20(8),* 14889-14901. https://doi.org/10.3390/molecules200814889

Holdbrook, D. A., Singh, S., Choong, Y. K., Petrlova, J., Malmsten, M., Bond, P. J., Verma, N. K., Schmidtchen, A., and Saravanan, R. (2018). Influence of pH on the activity of thrombin-derived antimicrobial peptides. *Biochimica et Biophysica Acta (BBA) – Biomembranes*, *1860*(11), 2374–2384. https://doi.org/10.1016/j.bbamem.2018.06.002

Kalle, M., Papareddy, P., Kasetty, G., Mörgelin, M., van der Plas, M. J., Rydengård, V., Malmsten, M., Albiger, B., and Schmidtchen, A. (2012). Host defense peptides of thrombin modulate inflammation and coagulation in endotoxin-mediated shock and *Pseudomonas aeruginosa* sepsis. *Plos One, 7*, Article e51313. https://doi.org/10.1371/journal.pone.0051313

Kasetty, G., Papareddy, P., Kalle, M., Rydengård, V., Mörgelin, M., Albiger, B., ... & Schmidtchen, A. (2011). Structure-activity studies and therapeutic potential of host defense

peptides of human thrombin. *Antimicrobial agents and chemotherapy*, *55*(6), 2880-2890. https://doi.org/10.1128/AAC.01515-10

Pane K., Durante L., Pizzo E., Varcamonti E., Zanfardino A., Sgambati V., …& Notomista E. (2016). Rational Design of a Carrier Protein for the Production of Recombinant Toxic Peptides in *Escherichia coli*. *PloS One, 11(1),* Article e0146552. https://doi.org/10.1371/journal.pone.0146552

Papareddy, P., Kalle, M., Kasetty, G., Mörgelin, M., Rydengård, V., Albiger, B., Lundqvist, K., Malmsten, M., and Schmidtchen, A. (2010). C-terminal peptides of tissue factor pathway inhibitor are novel host defense molecules. *Journal of Biological Chemistry*, *285*(36), 28387–28398. https://doi.org/10.1074/jbc.M110.127019

Papareddy, P., Rydengård, V., Pasupuleti, M., Walse, B., Mörgelin, M., Chalupka, A., ... & Schmidtchen, A. (2010). Proteolysis of human thrombin generates novel host defense peptides. *PLoS pathogens*, *6*(4), Article e1000857. https://doi.org/10.1371/journal.ppat.1000857

Petrlova, J., Hansen, F. C., Van Der Plas, M. J., Huber, R. G., Mörgelin, M., Malmsten, M., ... & Schmidtchen, A. (2017). Aggregation of thrombin-derived C-terminal fragments as a previously undisclosed host defense mechanism. *Proceedings of the National Academy of Sciences*, *114*(21), E4213-E4222. https://doi.org/10.1073/pnas.1619609114

Petrlova, J., Petruk, G., Huber, R. G., McBurnie, E. W., van der Plas, M. J., Bond, P. J., ... & Schmidtchen, A. (2020). Thrombin-derived C-terminal fragments aggregate and scavenge bacteria and their proinflammatory products. *Journal of Biological Chemistry*, *295*(11), 3417-3430. https://doi.org/10.1074/jbc.RA120.012741

Puthia, M., Butrym, M., Petrlova, J., Strömdahl, A. C., Andersson, M. Å., Kjellström, S., and Schmidtchen, A. (2020). A dual-action peptide containing hydrogel targets wound infection and inflammation. *Science Translational Medicine*, *12*(524), Article eaax6601. https://doi.org/10.1126/scitranslmed.aax6601

Rahim, K., Saleha, S., Zhu, X., Huo, L., Basit, A., Franco, O.L. (2017). Bacterial Contribution in Chronicity of Wounds. *Microbial Ecology*, *73*, 710-721. https://doi.org/10.1007/s00248-016-0867-9

van der Plas, M. J., Bhongir, R. K., Kjellström, S., Siller, H., Kasetty, G., Mörgelin, M., and Schmidtchen, A. (2016). *Pseudomonas aeruginosa* elastase cleaves a C-terminal peptide from human thrombin that inhibits host inflammatory responses. *Nature Communications*, *7*, Article 11567. https://doi.org/10.1038/ncomms11567

Widmaier, E. P., Raff H., Strang K. T. (2018). Cardiovascular Physiology. In Widmaier, E. P., Raff H., Strang K. T. (Eds.), *Human Physiology: The Mechanisms of Body Function* (15th ed., pp. 362-444). McGraw-Hill Education.

World Health Organization. (2020, July 31). *Antibiotic resistance.* https://www.who.int/news-room/fact-sheets/detail/antibiotic-resistance

Xia, X. (2007). *Bioinformatics and the Cell: Modern Computational Approaches in Genomics, Proteomics and Transcriptomics.* Springer. https://doi.org/10.1007/978-0-387-71337-3

9. Appendix

Calculation of protein yield after all purification steps

Protein concentration in fractions 1-3:
Fraction 1: 0.366 mg/mL × 0.5 mL = 0,18 mg
Fraction 2: 0.199 mg/mL × 0.5 mL = 0,10 mg
Fraction 3: 0.049 mg/mL × 0.5 mL = 0,02 mg

Total protein concentration after IMAC in fractions 1-3:
0,18 mg + 0,10 mg + 0,02 mg = 0,30 mg

Total concentration of protein after dialysis:
0,07 mg/mL × 3 mL = 0,21 mg

Amount of protein per 1 L of bacteria culture
0.5 L × 0.21 = 0.42 mg

Protein yield after dialysis:

$$Yield = \frac{concentration\ of\ rTCP96\ after\ dialysis}{concentration\ of\ rTCP96\ in\ fractions\ 1-3}$$

$Yield$ = 0,21/0,30 = 0,68

$Yield$ = 68 %